

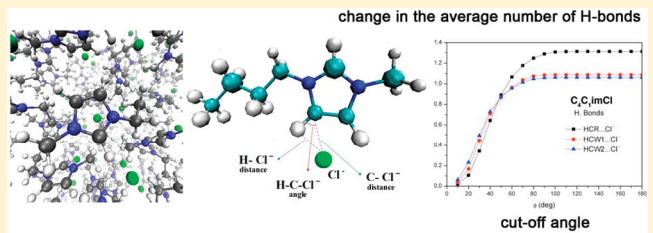
Hydrogen Bonding in 1-Butyl- and 1-Ethyl-3-methylimidazolium Chloride Ionic Liquids

Ioannis Skarmoutsos,*† Dimitris Dellis,‡ Richard P. Matthews,† Tom Welton,† and Patricia A. Hunt*,†

†Chemistry Department, Imperial College London, London SW7 2AZ, United Kingdom

‡Institute of Accelerating Systems and Applications, Panepistimiopolis Zografou, 15784 Athens, Greece

ABSTRACT: A detailed investigation of hydrogen bonding in the pure ionic liquids $[C_4C_1im]Cl$ and $[C_2C_1im]Cl$ has been carried out using primarily molecular dynamics techniques. Analyses of the individual atom–atom pair radial distribution functions, and in particular those for C···Cl⁻, have revealed that hydrogen bonding to the first methylene or methyl units of the substituent groups is important. Multiple geometric criteria for defining a hydrogen bond have been applied, and in particular the choice of the cutoff angle has been carefully examined. The interpretation of hydrogen bonding within these ionic liquids is highly angle dependent, and justification is provided for why it may be appropriate to employ a wider angle criteria than the 30° used for water or alcohol systems. The different types of hydrogen bond formed are characterized, and “top” conformations where the Cl anion resides above (or below) the imidazolium ring are investigated. The number of hydrogen bonds undertaken by each hydrogen atom (and the chloride anion) is quantified, and the propensity to form zero, one, or two hydrogen bonds is established. The effects of an increase in temperature on the static hydrogen bonding are also briefly examined.



I. INTRODUCTION

Ionic liquids (ILs) represent a very important class of solvents and electrolytes, and as such have a wide range of potential chemical and industrial applications.^{1–5} Key physical and chemical properties include a very low (almost zero) vapor pressure, high thermal conductivity and thermal stability, nonflammability, large electrochemical window, high polarity, and an ability to tune dissolving capability by selecting appropriate anion–cation pairs. These properties mean that ILs have the potential to be employed in a wide range of materials science and technological applications.^{1–16} However, the use of ILs as a reaction media or as electrolytes has been limited by suboptimal transport properties; ILs can be as viscous as oils.¹⁷ Thus, the design of new categories of ILs that exhibit low viscosity, high diffusivity, and high electrical and thermal conductivity is a key goal. These properties are dependent on interactions at the atomic scale, including those between the molecules and ions constituting the IL. The rational design of new ILs will be aided by a deeper and more quantitative understanding of the molecular level interactions occurring within ILs.

One of the crucial molecular level interactions affecting the physical and chemical properties of many liquids is hydrogen bonding (H-bonding).¹⁸ H-bonding involves complex attractive/repulsive intermolecular interactions of the type X–H···Y, where a hydrogen atom intercedes between two species X and Y. A typical criterion for determining the presence of a hydrogen bond is that the distance between X and Y should be less than the sum of the van der Waals radii; however, this has been criticized as too limiting.¹⁹ Another criterion has been the

directionality of the H-bond: the angle $\theta(X-H\cdots Y)$ should be close to linear or 180°; however, this criterion has also been recognized as limiting particularly in the case of blue-shifted or weak H-bonds.¹⁹ Nevertheless, simple geometric criteria of this type are favored because they can be readily obtained from structural information, for example, X-ray data and neutron diffraction data, or from analysis of molecular dynamics trajectories. In addition, the dynamic properties of hydrogen bonds so defined can be easily determined. More complex definitions of H-bonding include formulations based on energies, potential energy surfaces, and/or the electron density; IUPAC has also recently released a technical report on defining the H-bond.¹⁹

Recent theoretical^{20–22,26–43} and experimental studies^{22,23,25,44–59} have probed H-bonding in ILs; however, the nature of these H-bonds and how they affect the properties of ILs is still a key area of debate. Moreover, H-bonds in different ILs can vary widely. There is no firm commonly accepted definition of a H-bond, and in an IL the H-bond becomes extremely difficult to clearly characterize. In the context of the difficulty of defining a H-bond in normal molecular liquids, and the additional complexity of defining a H-bond for ionic liquids where the Coulombic interactions of the ions cannot be easily separated from the Coulombic component associated with H-bonding, the definition employed can be a matter of semantics.

Received: October 1, 2011

Revised: March 8, 2012

Published: April 16, 2012

Nevertheless, analysis of structural information can provide insight.

Molecular simulation studies of ILs typically employ geometric criteria to define the presence of a H-bond.^{24,29,31} Cation–anion radial distribution functions do not have the detailed atomic resolution required and can vary qualitatively depending on the origin defined (for example, geometric center-of-mass or center of the ring for imidazolium based cations).²⁹ However, atom site-to-site pair radial distribution functions (prdf) can offer useful information. Typically criteria for H-bonds have been based on those derived from H-bonding in neutral molecular liquids such as water and alcohols.^{60,61} For example, it is usual to define a H-bond when the O···O distance is less than the first minima in the O···O prdf $g_{OO}(r)$. Further refinements can include a requirement that the angle $\phi(O\cdots O-H)$ does not deviate strongly from 0° and/or a second distance criterion based on the O···H prdf $g_{OH}(r)$. There are two common angle definitions $\theta(X-H\cdots Y)$ where the H-bond angle is close to linear (180°) or equivalently $\phi(Y\cdots X-H)$ where the H-bond angle is close to 0° ; the second definition will be employed in this work. Common conditions for the presence of H-bonds in water, methanol, or ethanol from molecular dynamics simulations are O···O distances smaller than 3.5 Å, O···H distances smaller than 2.6 Å, and an angle HO···O smaller than 30° .^{60,61} Multiple constraint definitions of the H-bond have been found particularly useful for describing H-bonding in liquid and supercritical water.^{62,63}

One of the main aims of this work is to investigate in detail, using multiple constraint geometric conditions, H-bonding in two specific ILs: 1-butyl-3-methylimidazolium chloride [C_4C_1im]Cl (BmimCl) and 1-ethyl-3-methylimidazolium chloride [C_2C_1im]Cl (EmimCl). The question arises as to how transferable to IL are typical H-bonding criteria? The nature of the H-bond formed in ILs appears to be very different from that formed in molecular liquids. ILs are composed of cations and anions while molecular liquids (such as water, peptides, or alcohols) are composed of neutral molecules. In particular, the transferability of an angle criterion of 30° from molecular liquids to ILs is of interest. The effect of temperature on the static H-bonding network of these ILs will also be considered.

The H-bonds that form between the chloride anion and imidazolium cation can be partitioned into three main types based on the position of the relevant hydrogen atoms, Figure 1. The three hydrogen atom types can also be grouped by atomic partial charge (on each H atom) and the computed C–H vibrations.^{21,35} The first type we denote “ring” hydrogen atoms; these are hydrogen atoms in the imidazolium ring, HCR (primary), and HCW1 and HCW2 (ring). The second type are denoted “first” hydrogen atoms, those closest to the ring; first in the attached substituent groups, HMe (methyl), and HC1 (the first methylene group of the butyl or ethyl chain). The third type are denoted “alkyl” hydrogen atoms and include all the remaining alkyl group hydrogen atoms on the butyl or ethyl chains. A potential fourth type of interaction is also very important; this occurs when the chloride anion is positioned “above” or “below” the imidazolium ring. This interaction has not yet been fully characterized but impacts on the H-bonding in imidazolium based ILs with strong H-bonding anions.

Many studies of imidazolium based ILs have considered H-bonding; these include experimental,^{54,58,59} classical molecular dynamics,^{29a} ab initio molecular dynamics,^{29b} and quantum chemical studies.^{21,32,35,43,54,59} Most studies have focused on

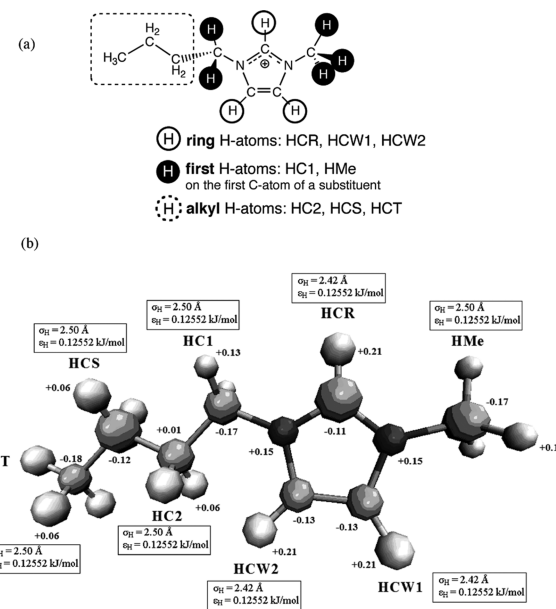


Figure 1. (a) Scheme of H-atom types, (b) naming convention, key point charges, and Lennard-Jones parameters used in the [C_4C_1im] (Bmim) and [C_2C_1im] (Emim) cation potentials.

the primary-ring H-bonding interaction, that of the anion with HCR, while some have also mentioned the other ring hydrogen atoms. However, weaker secondary interactions with the first hydrogen atoms are possible and have been considered in relatively few cases, particularly in the case of the methyl substituent.^{21,29a,31,43} When a H-bond network forms, these interactions play an important role. Moreover, in the liquid state these secondary interactions additionally stabilize the primary H-bond configurations, and as the temperature increases more structures above the minimum energy configuration will be sampled. Thus, a full range of H-bonding interactions has been investigated here. A key aim of this study has been to provide quantitative estimations of the number of H-bonds undertaken by each type of hydrogen atom, as well as quantitative estimations for the H-bonding undertaken by the Cl anion.

As with all MD studies, the results are dependent on the quality of the potential. A few studies have been undertaken in which H-bonding structural parameters from various classical MD simulations have been compared with ab initio MD.^{29c,d} Differences in the H-bonding distances and angle distributions have been observed and are clearly illustrated in Figure 4 of ref 29d. Such comparisons are not straightforward because the ab initio MD simulations are carried out with small cells, use gradient corrected but not hybrid functionals, and do not recover dispersion effects and the simulations may not be reaching equilibration. However, it is also clear that the H-bonding and angle distributions of classical MD simulations are potential dependent (even to reasonably subtle changes in atomic charge).^{29c}

This paper is organized as follows: the computational details are presented in section II; results and discussion are presented in section III; general conclusions are presented in section IV.

II. SIMULATION DETAILS

In the present study simulation runs were performed for [C_4C_1im]Cl and [C_2C_1im]Cl, at constant temperature and volume using the DL_POLY simulation code.⁶⁴ To the best of

our knowledge, reliable experimental data of liquid densities for these systems are relatively scarce; thus, two previously reported experimental state points have been simulated. $[C_4C_1im]Cl$ has been simulated at a thermodynamic state (1052.8 kg m^{-3} , 353.15 K)^{65,66} close to its melting point ($T_m = 340.1 \text{ K}$)^{67,68} and $[C_2C_1im]Cl$ at thermodynamic conditions (1040.0 kg m^{-3} , 450.0 K)⁶⁹ well above its melting temperature ($T_m = 360.0 \text{ K}$).⁷⁰ In order to confirm temperature effects, $[C_2C_1im]Cl$ was also simulated at a lower temperature, slightly above its melting point (363 K) at the corresponding experimental density.⁶⁹

The simulations were carried out using 128 pairs of anions and cations in the central simulation box. Starting structures were generated after energy minimization of a crystal structure followed by equilibration at a higher temperature and then controlled cooling. Equilibration simulations of 5 ns were initially performed for each liquid. Properties were then evaluated from three sequential 5 ns simulations, and thus the total simulation time is 20 ns. The equations of motion were integrated using a leapfrog-type Verlet algorithm, and the integration time step was set to 1 fs.⁷¹ A Nose–Hoover thermostat with a temperature relaxation time of 0.2 ps was used to constrain the temperature during simulations.⁷² The intramolecular geometry was constrained using a modified version of the SHAKE algorithm.^{73,74}

The chemical structure (and atomic labeling) of the $[C_4C_1im]$ and $[C_2C_1im]$ cations is indicated in Figure 1. The potential model of Lopes and Padua has been employed to describe site–site interactions, and corrections made by the authors in the Supporting Information of a later publication have been taken into account.^{75,76} The intermolecular interactions are represented as pairwise additive with site–site Lennard-Jones plus Coulomb interactions. The intramolecular interactions have been represented in terms of harmonic bond stretching and angle bending, as well as a cosine series for dihedral angle internal rotations. A cutoff radius of 12.0 Å has been applied for all Lennard-Jones interactions, and long-range corrections have been also taken into account. To account for the long-range electrostatic interactions, the standard Ewald summation technique has been used.

III. RESULTS AND DISCUSSION

A. Local Hydrogen Bonding Structure. The site to site pair radial distribution functions used to investigate H-bonding in water and alcohols relate to O···O and O···H distances and to deviation of the HO···O angle from 0° . In this section the corresponding analogues for $[C_4C_1im]Cl$ and $[C_2C_1im]Cl$ are examined; they include C···Cl⁻ and H···Cl⁻ distances and the HC···Cl⁻ angle, Figure 2. In addition to the dominant and primary H-bond formed with HCR, the potential for H-

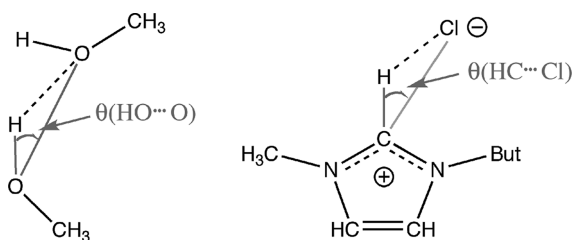


Figure 2. Typical bond distances and angles used to define hydrogen bonding for methanol and the analogous parameters for $[C_4C_1im]Cl$.

bonding with the other ring, first, and alkyl chain hydrogen atoms is examined in detail. For ILs it has been typical to consider the H···Cl⁻ prdfs with only occasional and minor consideration of the C···Cl⁻ prdfs; thus, H-bonding from a perspective of the C···Cl⁻ prdfs is also examined in more detail.

The H···Cl⁻ prdfs for $[C_4C_1im]Cl$ and $[C_2C_1im]Cl$ are presented in Figures 3 and 4. Our results are consistent with

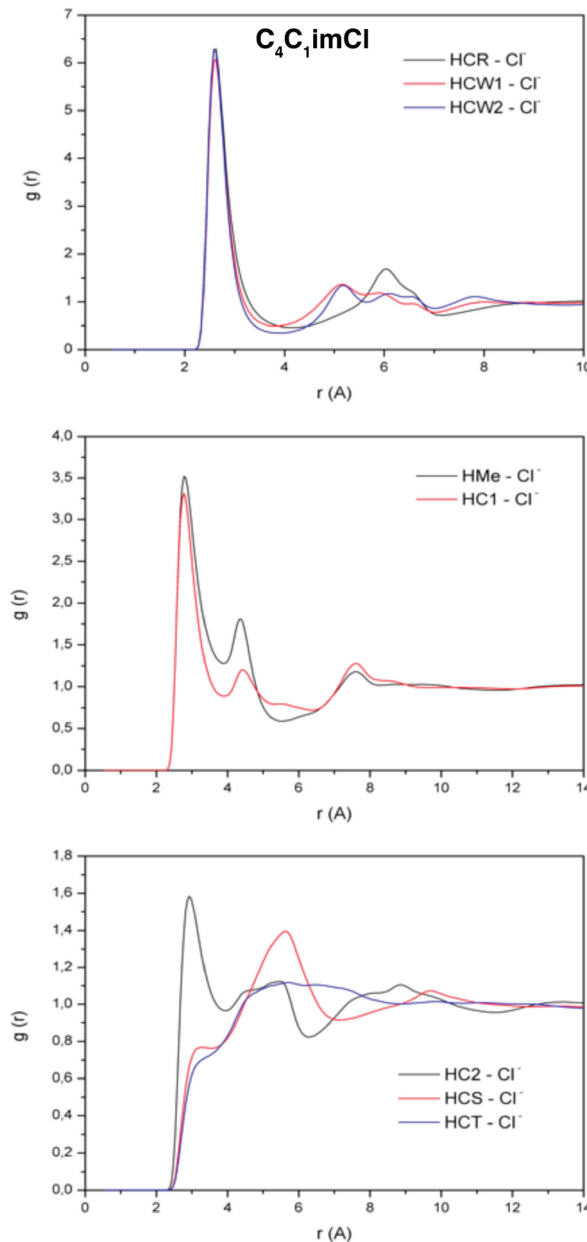


Figure 3. Calculated H···Cl⁻ site–site radial distribution functions for $[C_4C_1im]Cl$.

the established picture for these ILs. For example, there are clear differences between the ring, first, and alkyl hydrogen atom prdfs. The intensities of the first peak maxima of the H···Cl⁻ prdfs decrease with distance of the hydrogen atom from the imidazolium ring; moreover, the alkyl chain hydrogen atom prdfs exhibit only a weak shoulder around 2.5 Å and an enhanced probability at larger distances. Thus, there is a much higher probability of finding a chloride anion near the ring than an alkyl chain. This is consistent with the charge distribution in

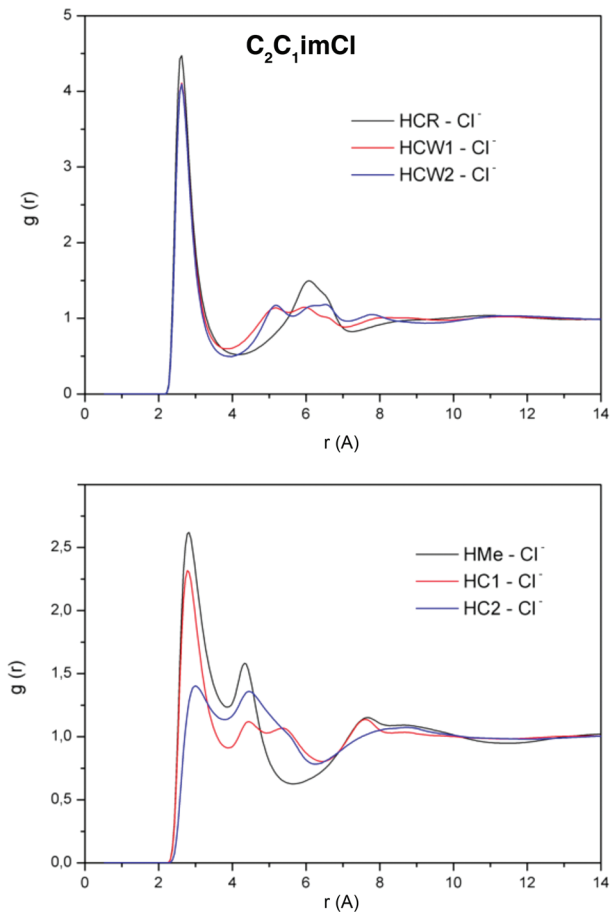


Figure 4. Calculated $\text{H}\cdots\text{Cl}^-$ site–site radial distribution functions for $[\text{C}_2\text{C}_1\text{im}]\text{Cl}$.

the potential employed for these simulations, Figure 1, ring (+0.21), first (+0.13), and alkyl (+0.06) hydrogen atoms, respectively. The prdfs for the first hydrogen atoms, $\text{C}1\text{H}\cdots\text{Cl}^-$ and $\text{MeH}\cdots\text{Cl}^-$, have a double peak structure with the second peaks occurring at 4.43 and 4.38 Å, respectively. The first peak of the ring and first hydrogen atom prdfs can relate to the same Cl anion, while the second peak can be associated with a different Cl anion, one that is primarily stabilized by a stronger H-bonding interaction with a second cation Figure 5.

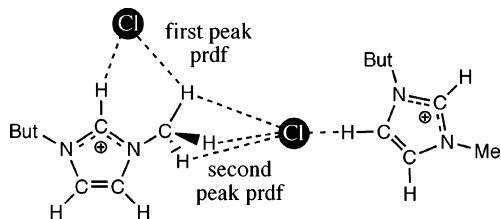


Figure 5. Cartoon representing the type of interaction giving rise to the second peak in the first hydrogen atom prdfs.

The $\text{C}\cdots\text{Cl}^-$ prdfs for $[\text{C}_4\text{C}_1\text{im}]\text{Cl}$ and $[\text{C}_2\text{C}_1\text{im}]\text{Cl}$ are presented in Figures 6 and 7. In contrast to the $\text{H}\cdots\text{Cl}^-$ prdfs in which the imidazolium ring hydrogen atoms have similar first peak intensities, the $\text{CR}\cdots\text{Cl}^-$ primary peak intensity is higher than the other ring carbon atoms, and this is consistent with the Cl anion taking up positions above or below at the front but not at the rear of the imidazolium ring. For the potential

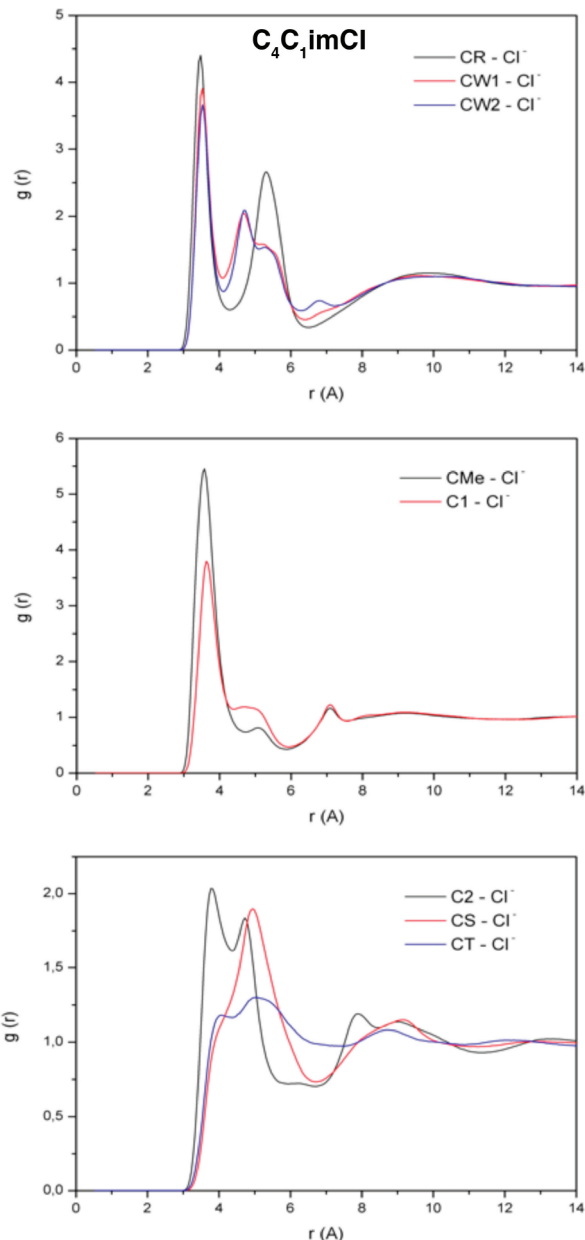


Figure 6. Calculated $\text{C}\cdots\text{Cl}^-$ site–site radial distribution functions of $[\text{C}_4\text{C}_1\text{im}]\text{Cl}$.

employed in these simulations, CR is negatively charged (-0.11) while the nitrogen atoms are positively charged ($+0.15$). Thus, the locality of the anion around CR, for this classical potential, may be based more on a Coulombic attraction to the nitrogen atoms than to the CR carbon atom. Ab initio electronic density derived charge analysis places more emphasis on the CR as a positively charged species and the electronegative nitrogen atoms as negatively charged species and would favor a more direct interaction with CR.⁴³ Both classical and ab initio methods clearly indicate that the out-of-plane interaction impacts on the liquid structure.

The interaction of the methyl group with Cl anions is well-known from spacial distribution functions.^{29d} However, the first peak intensity of the $\text{CMe}\cdots\text{Cl}^-$ prdf is higher than the other prdfs, and this result was unexpected as the CR interaction was anticipated to be the strongest. Although CMe (-0.17) is more negatively charged than CR, it is also bound to three positively

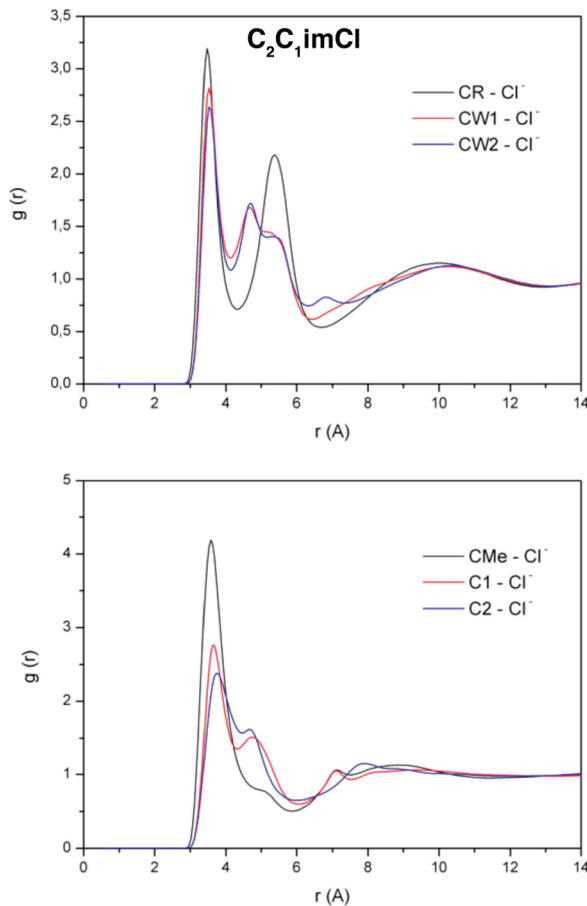


Figure 7. Calculated C...Cl⁻ site–site radial distribution functions of [C₂C₁im]Cl.

charged hydrogen atoms which can each act to draw in the anion. Thus, while the individual H...Cl⁻ prdfs highlight specific hydrogen based interactions, the C...Cl⁻ prdfs offer valuable information regarding the methyl/methylene units acting as a “group”. A key new insight obtained from our data (and developed further shortly) is that the first methylene and methyl groups have an impact comparable to the primary H-bonding interaction.

B. Distance Based Criteria for Defining Hydrogen Bonding. Typically molecular dynamics studies on the H-bonding properties of ILs have used the donor–acceptor distance H...X⁻ (X = Cl⁻, F⁻, etc.) as the only H-bonding criterion.^{24,28,29,31} However, recent theoretical studies have revealed the importance of the C...X⁻ interactions in properly describing H-bonding in ILs.⁴² This has also been re-enforced by our analysis of the C...Cl⁻ prdfs above. Thus, in addition to the H...Cl⁻ criteria, C...Cl⁻ cutoff distances have been employed. The radial distances to the first minimum for each *individual* hydrogen H...Cl⁻ and carbon C...Cl⁻ prdf are presented in Table 1. These numbers provide a dual geometric cutoff distance for determining the presence of a H-bond. Coordination numbers obtained via integrating up to the first minimum and corresponding to the number of H-bonds formed have also been computed and show a complex behavior, Table 1.

The ring and first hydrogen atoms all show an average coordination number greater than one, indicating that each hydrogen atom spends some time interacting with two anions

Table 1. Position of the First Minima for the H...Cl⁻ and C...Cl⁻ Radial Distribution Functions (Å) of [C₄C₁im]Cl and [C₂C₁im]Cl and the Calculated Coordination Numbers

	$r_{\text{cut}}(\text{H}\cdots\text{Cl}^-)$ (Å)	N_C	$r_{\text{cut}}(\text{C}\cdots\text{Cl}^-)$ (Å)	N_C
[C ₄ C ₁ im]Cl				
HCR	4.13	1.40	4.23	1.38
HCW1	3.78	1.15	4.08	1.21
HCW2	3.88	1.12	4.13	1.16
HMe	3.88	1.35	4.73	2.62
HC1	3.88	1.11	4.38	1.70
HC2	3.93	0.80	4.38	1.22
HCS	3.23	0.16	4.13	0.40
HCT	3.43	0.21	4.38	0.70
[C ₂ C ₁ im]Cl				
HCR	4.18	1.45	4.33	1.46
HCW1	3.88	1.21	4.13	1.27
HCW2	3.98	1.20	4.13	1.19
HMe	3.88	1.35	4.93	2.94
HC1	3.88	1.10	4.33	1.63
HC2	3.83	0.88	4.48	1.87

simultaneously in a bifurcated H-bond. For the ring hydrogen atoms bifurcated H-bonds to multiple F atoms (on the same anion) have previously been found in [C₄C₁im][PF₆].²⁸ However, because the Cl anion is a single atom, the bifurcated bond must be to two separate anions, enhancing the H-bond interconnectivity for these ILs and potentially contributing to a higher melting point.

Coordination numbers for the substituent methyl group are almost as large as those for the primary hydrogen atom. This effect is magnified when the number of hydrogen atoms is taken into consideration, one in the case of HCR and three for the methyl group. This trend is also re-enforced by the C...Cl⁻ coordination numbers; for example, there are 1.38 close contacts for the primary ring C...Cl⁻ and 2.62 for the methyl substituent in [C₄C₁im]Cl.

On the basis of the occurrence and importance of MeH...Cl⁻ interactions derived from the molecular dynamics studies (MeH...Cl⁻ and MeC...Cl⁻ prdfs and coordination numbers), the potential existence of an ion-pair structure of this type was further investigated using ab initio quantum chemical techniques (technical details are presented shortly). Previous ab initio studies have not typically looked for such high energy structures.^{29b,32b,42} A stable ion-pair structure has been found nearly 100 kJ/mol higher in energy than the most stable ion-pair; thus, this structure would not persist in isolation. However, the motif must provide some small amount of stabilization; otherwise, it would not be observed in the liquid. The MeH...Cl⁻ interaction may form in preference to other more stable interactions (i.e., with ring hydrogen atoms) because the methyl group is more accessible (sterically as the methyl is on the periphery of the molecule, or kinetically there may be an energy barrier to accessing other more stable sites).

Hydrocarbon interactions are dominated by closed shell dispersive interactions, and so the MeH...Cl⁻ interaction could be expected to have a large dispersive component; thus, we employed a standard functional B3LYP/6-311+G(d,p), a dispersion corrected functional B97D/aug-cc-pVTZ, and the highest method employed here: MP2/6-311+G(d,p). A structure was located at the B3LYP/6-311+G(d,p) level 90.91 kJ/mol above the lowest energy conformer; however, the lowest energy vibration is essentially 0 cm⁻¹. The dispersion

corrected functional did not locate a minimum, but the MP2/6-311+G(d,p) method did converge to a verified minima. Clearly recovering this interaction is highly method and basis set dependent and does not appear to be purely a product of dispersion (since the standard B3LYP method, which does not include dispersion, found a minima).

Thus, the important result here is that, based on the C \cdots Cl $^-$ prdf analysis, the first methylene and methyl groups have a higher coordination number (with the Cl anions) than the primary C–H, indicating they play an important secondary stabilizing and networking role within the IL.

C. The Importance of Directionality for IL Hydrogen Bonding. Multiple constraint definitions including a directionality component have been found useful for developing an understanding of H-bonding in other liquids. Thus, the use of a H-bonding angle criteria has been explored here, where the angle $\phi(\text{Cl}^- \cdots \text{C}-\text{H})$ is less than or equal to a specified cutoff value. A number of previous publications have employed a cutoff angle 30°,^{24,29,31} following similar definitions for water and alcohols.^{60,61} An in-depth theoretical study of H-bonding in ILs has shown that bond angles involving a hydrogen atom can vary widely, some showing directionality while others do not.^{29b,42} In this section the detailed effects of the angular criteria on H-bonding in [C₄C₁im]Cl and [C₂C₁im]Cl are examined for the first time.

H-bonds are first selected based on distance criteria; $R_{\text{H}\cdots\text{Cl}}$ and $R_{\text{C}\cdots\text{Cl}}$ must both lie within their respective cutoff distances (first minima of the pdrfs defined in Table 1). The probability density distributions $f(\phi)$ of angles ϕ with values between $\phi + d\phi/2$ and $\phi - d\phi/2$ for [C₄C₁im]Cl and [C₂C₁im]Cl are presented in Figures 8 and 9, respectively. The area under the calculated curves has been normalized to unity. These graphs represent the distribution of angles for H-bonding if no angular criteria are applied. The position of the peak maximum λ and the average angle $\langle\phi\rangle$ are presented in Table 2.

The ring hydrogen atoms exhibit a peak between 28° and 34° while the mean angle is slightly larger, between 34° and 45°. Compared to the other ring hydrogen atoms, the primary hydrogen has an angle distribution shifted to slightly higher angles, consistent with the Cl anion out-of-plane interaction conformers. However, the first hydrogen atoms exhibit a peak, and average angle at even higher values, and the distributions are wider, particularly so for the first methyl hydrogen atoms, resulting in mean angle values of 53.5° and 52.5° for [C₄C₁im]Cl and [C₂C₁im]Cl, respectively. This can be rationalized on the basis of a primary interaction dominating the angle distribution and the first hydrogen atom interactions, being weaker, delivering a secondary level of stabilization. The strong draw of the primary interaction pulls the anion away from the local minimum of a relatively shallow potential energy surface around the first hydrogen atom, inducing a larger mean angle.

The back ring hydrogen atoms, and to a lesser extent the primary and first hydrogen atoms, exhibit a distinct shoulder around 60°, and an inflection point can be determined. Such an inflection point has been observed at $\approx 30^\circ$ in the case of liquid water and alcohols, and 30° is the angle that has successfully been employed as a cutoff for H-bonding in such systems. The inflection point at $\approx 30^\circ$ has been verified by calculating the second order derivatives of the cutoff angle distributions of water and ethanol from previous calculations by one of the authors.^{77,78}

Clearly an angular cutoff of 30° is less than the average angle and does not always include the peak maximum for these

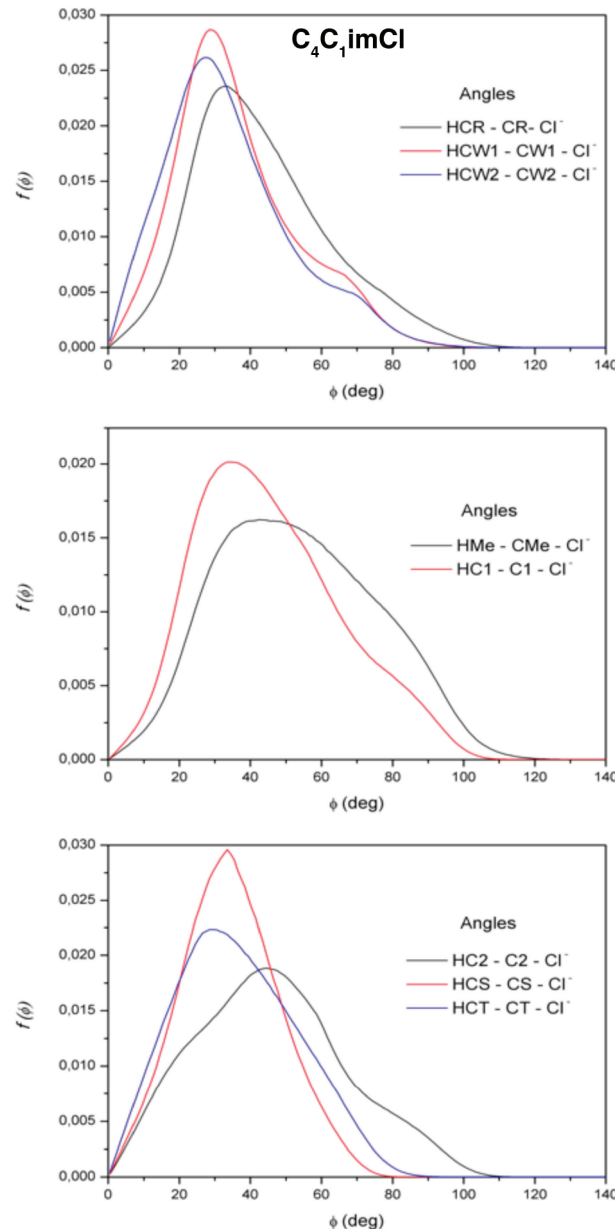


Figure 8. Distribution of angles $\phi(\text{Cl}^- \cdots \text{C}-\text{H})$ for atoms within the cutoff distances $R_{\text{H}\cdots\text{Cl}}$ and $R_{\text{C}\cdots\text{Cl}}$ for [C₄C₁im]Cl.

distributions. Moreover, these distributions are skewed to higher angles, particularly those for the ring hydrogen based interactions. Thus, a cutoff criterion of 30° excludes a significant proportion of interactions lying within the distance based criteria. Consequently we have explored the H-bonding characteristics of these ILs using a range of angular cutoff values and focusing particularly on those at 30° and 60°, and the results are presented and discussed in the next section.

D. The Effect of Employing Different Angle Based Criteria on Hydrogen Bonding. Employing the radial cutoffs presented in Table 1 and an angular cutoff of 30° and 60°, the average number of H \cdots Cl $^-$ H-bonds per each hydrogen type atom in [C₄C₁im]Cl and [C₂C₁im]Cl has been calculated, Table 3, and additional values for a 120° angular cutoff are also presented for the ring hydrogen atoms.

A key feature emerging from the analysis is that changing the cutoff angle significantly changes the way in which the H-

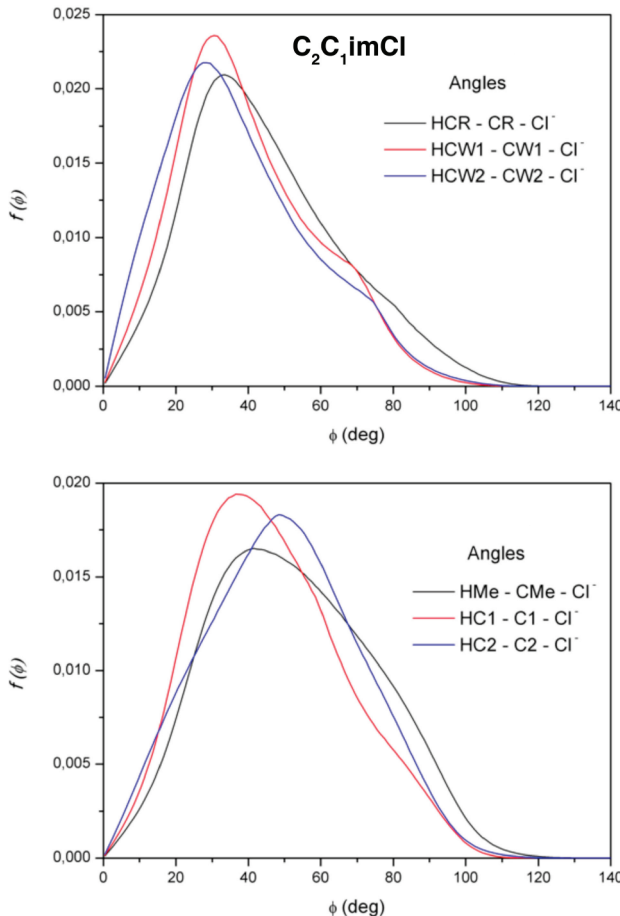


Figure 9. Distribution of angles $\phi(\text{Cl}^- \cdots \text{C}-\text{H})$ for atoms within the cutoff distances $R_{\text{H}\cdots\text{Cl}}$ and $R_{\text{C}\cdots\text{Cl}}$ for $[\text{C}_2\text{C}_1\text{im}]\text{Cl}$.

Table 2. Position of the Peak Maxima λ and the Mean Angle $\langle\phi\rangle$ (in deg) for the Angle Distributions $\phi = \text{H}-\text{C}\cdots\text{Cl}^-$ for $[\text{C}_4\text{C}_1\text{im}]\text{Cl}$ and $[\text{C}_2\text{C}_1\text{im}]\text{Cl}$

	$[\text{C}_4\text{C}_1\text{im}]\text{Cl}$		$[\text{C}_2\text{C}_1\text{im}]\text{Cl}$	
	λ (°)	$\langle\phi\rangle$ (°)	λ (°)	$\langle\phi\rangle$ (°)
HCR	33.5	43.4	33.5	44.9
HCW1	28.5	36.3	30.5	40.0
HCW2	27.5	34.0	28.5	38.0
HMe	42.5	53.5	41.5	52.5
HC1	34.5	45.5	36.5	46.2
HC2	44.5	46.0	48.5	49.4
HCS	33.5	34.6	—	—
HCT	29.5	36.4	—	—

^aAll atoms lie within the cutoff distances for $R_{\text{H}\cdots\text{Cl}}$ and $R_{\text{C}\cdots\text{Cl}}$.

bonding can be interpreted. For example, in $[\text{C}_4\text{C}_1\text{im}]\text{Cl}$ using a cutoff of 30° most of the primary ring hydrogen atoms are *H-bond free* (coordination number 0.34). In addition, the hydrogen atoms at the back of the ring experience more H-bonding than the primary hydrogen atom, coordination numbers 0.45 and 0.50. This is surprising, as we expected the strongest H-bond donor to be almost entirely involved in H-bonding in solution. Theoretical ab initio^{20,21,32,38,43,54,59} and experimental^{50,54,58,59,79–81} studies indicate that the front hydrogen atom of the ring (HCR) undertakes the primary H-bonding interaction and has a more acidic character than the other ring hydrogen atoms. When using a cutoff of 60° , a

Table 3. Average Numbers of $\text{H}\cdots\text{Cl}^-$ Hydrogen Bonds $\langle n_{\text{HB}} \rangle$ for Each Hydrogen Atom Type Using Angular Cutoffs of 30° and 60° and for the Ring Hydrogen Atoms at 120° for $[\text{C}_4\text{C}_1\text{im}]\text{Cl}$ and $[\text{C}_2\text{C}_1\text{im}]\text{Cl}$

	$[\text{C}_4\text{C}_1\text{im}]\text{Cl}$			$[\text{C}_2\text{C}_1\text{im}]\text{Cl}$		
	30°	60°	120°	30°	60°	120°
HCR··· Cl^-	0.34	1.07	1.31	0.35	1.03	1.34
HW1··· Cl^-	0.45	0.96	1.09	0.38	0.92	1.10
HW2··· Cl^-	0.50	0.96	1.06	0.42	0.89	1.06
HMe··· Cl^-	0.20	0.83	—	0.22	0.85	—
HC1··· Cl^-	0.26	0.80	—	0.23	0.75	—
HC2··· Cl^-	0.17	0.51	—	0.16	0.55	—
HCS··· Cl^-	0.06	0.14	—	—	—	—
HCT··· Cl^-	0.08	0.18	—	—	—	—

significant fraction of the primary hydrogen atoms form at least one H-bond (coordination number 1.07) and the “primary” hydrogen becomes the primary H-bond donor (the coordination number for the back of the ring hydrogen atoms is 0.96). Thus, employing the higher angular cutoff recovers the generally accepted picture of H-bonding in these ILs. As a corollary, increasing the angular cutoff also significantly increases the average number of H-bonds to the first hydrogen atoms relative to the ring hydrogen atoms.

The significant changes in H-bonding observed on changing the angle cutoff have been further investigated for the primary hydrogen atoms, Figure 10. The mean number of H-bonds increases until a plateau is reached at 120° ; this value is the number of H-bonds that will be obtained using only the distance based criteria without angular restrictions.

The average number of H-bonds per cation can be estimated by summing up the average number of H-bonds formed for each hydrogen atom in the cation. When using a 30° cutoff for $[\text{C}_4\text{C}_1\text{im}]\text{Cl}$, this is estimated to be 3.11, and for 60° the average is three times higher at 8.92. (The corresponding numbers for $[\text{C}_2\text{C}_1\text{im}]\text{Cl}$ are 2.75 and 8.54, respectively.) Crystal structures of the two polymorphs of $[\text{C}_4\text{C}_1\text{im}]\text{Cl}$ show contact with six and seven anions.⁷⁹ Neutron diffraction of $[\text{C}_1\text{C}_1\text{im}]\text{Cl}$ shows six anions within the first radial cutoff of the cation–anion rdf.⁵⁶ Thus, only one or possibly two Cl anions need to contribute to a bifurcated H-bond to reach the numbers of H-bonds per cation associated with the 60° cutoff value.

The density of ions in these ILs mean that a single hydrogen atom can interact with more than one Cl anion at the same time. To investigate the proportion of hydrogen atoms undertaking multiple H-bonding interactions, the fraction of ring hydrogen atoms having 0, 1, and 2 H-bonds for three different angular cutoffs (30° , 60° , and 120°) has been determined, Table 4 ($[\text{C}_4\text{C}_1\text{im}]\text{Cl}$) and Table 5 ($[\text{C}_2\text{C}_1\text{im}]\text{Cl}$). The fraction of all hydrogen atom types having 0, 1, and 2 H-bonds for a 60° cutoff are presented in Table 6.

When a cutoff angle of 30° is employed (Table 4), the primary ring hydrogen atoms are (again) on average H-bond free. In addition, no primary hydrogen atoms form more than one H-bond. When employing a cutoff angle of 60° , the ring hydrogen atoms are involved in H-bonds, and a small proportion are involved in multiple H-bonds: 11% for the primary hydrogen atoms. In addition, about 70% of the first hydrogen atoms also participate in one H-bond, and a small proportion participate in two H-bonds ($\approx 5\%$).

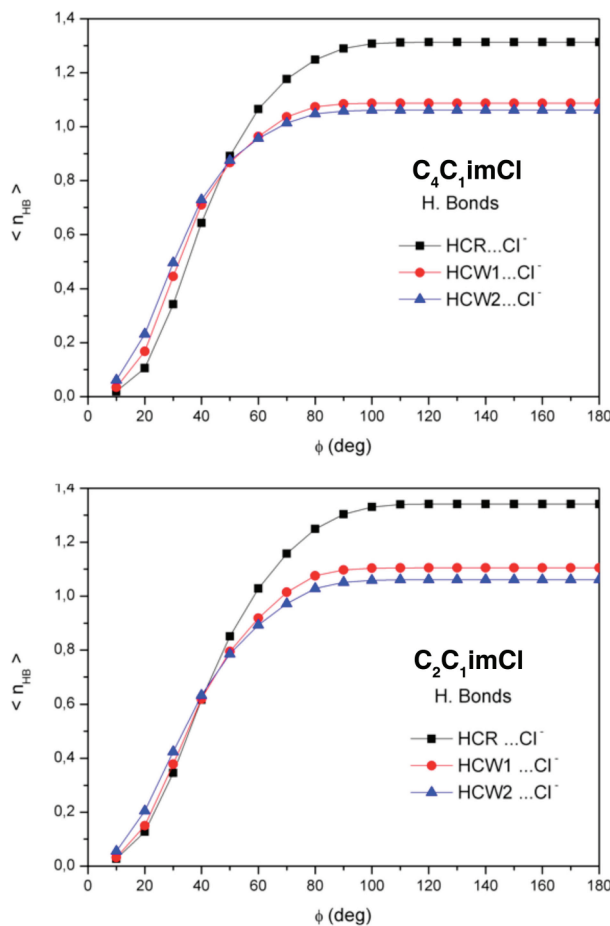


Figure 10. Change in the mean number of hydrogen bonds with angle cutoff for the ring hydrogen atoms in $[C_4C_1\text{im}]Cl$ and $[C_2C_1\text{im}]Cl$.

Table 4. Average Percentage of $[C_4C_1\text{im}]$ Imidazolium Ring Hydrogen Atoms Forming $n = 0\text{--}2$ Hydrogen Bonds^a

	0-HB (%)	1-HB (%)	2-HB (%)
HCR...Cl ⁻			
30°	65.77	34.23	0.00
60°	4.48	84.53	10.99
120°	1.00	66.84	32.16
HCW1...Cl ⁻			
30°	55.42	44.58	0.00
60°	7.83	87.96	4.21
120°	4.35	82.68	12.97
HCW2...Cl ⁻			
30°	50.36	49.64	0.00
60°	7.00	90.31	2.69
120°	3.91	86.08	10.01

^aResults are depicted for different angular cutoffs.

In section C we established that the bulk of the angular distribution is excluded when employing a cutoff of 30° (given both distance criteria $R_{H\cdots Cl}$ and $R_{C\cdots Cl}$ are satisfied). In this section we established that to be consistent with the generally accepted picture of imidazolium cations primarily acting as a H-bond donor through the HCR hydrogen atom, it is important to consider a higher cutoff angle such as 60°. Figure 10 shows there is a dramatic change in H-bonding coordination number with changing cutoff angle. Thus, it is clear that the qualitative interpretation H-bonding changes significantly with cutoff

Table 5. Average Percentage of $[C_2C_1\text{im}]$ Imidazolium Ring Hydrogen Atoms Forming $n = 0\text{--}2$ Hydrogen Bonds^a

	0-HB (%)	1-HB (%)	2-HB (%)
HCR...Cl ⁻			
30°	65.44	34.56	0.00
60°	6.72	83.70	9.58
120°	1.50	63.08	35.42
HCW1...Cl ⁻			
30°	62.18	37.82	0.00
60°	12.44	83.28	4.28
120°	6.47	76.67	16.86
HCW2...Cl ⁻			
30°	57.56	42.44	0.00
60°	13.94	82.81	3.25
120°	7.83	78.32	13.85

^aResults are depicted for different angular cutoffs.

Table 6. Average Percentage of Hydrogen Atoms Forming $n = 0\text{--}2$ Hydrogen Bonds, Using an Angular Cutoff of 60°

	0-HB (%)	1-HB (%)	2-HB (%)
$[C_4C_1\text{im}]Cl$			
HCR...Cl ⁻	4.48	84.53	10.99
HW1...Cl ⁻	7.83	87.96	4.21
HW2...Cl ⁻	7.00	90.31	2.69
HMe...Cl ⁻	22.87	71.65	5.48
HC1...Cl ⁻	22.98	73.70	3.32
HC2...Cl ⁻	49.55	49.65	0.80
HCS...Cl ⁻	85.53	14.46	0.01
HCT...Cl ⁻	82.52	17.45	0.03
$[C_2C_1\text{im}]Cl$			
HCR...Cl ⁻	6.72	83.70	9.58
HW1...Cl ⁻	12.44	83.28	4.28
HW2...Cl ⁻	13.94	82.81	3.25
HMe...Cl ⁻	21.42	72.57	6.01
HC1...Cl ⁻	28.43	68.36	3.21
HC2...Cl ⁻	46.80	51.41	1.79

angle, and analyzing just one cutoff angle can give an incomplete picture of the H-bonding in these ILs.

E. The Cl Anion as a Hydrogen Bond Acceptor. The analysis presented so far has been focused on the cation as a H-bond donor. The other half of this interaction includes the Cl anion as a H-bond acceptor, one that can form multiple H-bonding interactions. Using the previously employed criteria for bond distances and an angle cutoff of 60°, the fraction of Cl anions forming 0–5 H-bonds with each type of hydrogen atom have been computed, Table 7. The information in this table is Cl anion “centric”; for example, on average 27% of Cl anions form no interaction with any primary hydrogen (HCR), 44% form one H-bonding interaction, and 23% form interactions with two different primary hydrogen atoms (additional interactions can also form; this number recovers only interactions with the specified type of hydrogen atom).

On average 41% of Cl anions form a H-bond interaction with HC2, an alkyl chain hydrogen atom. This may not initially seem very sensible; however, ab initio studies of the stable minima for the Cl anion show interactions of this hydrogen atom with the anion, Figure 11.⁴³

Examination of the columns for two and three H-bonds (Table 7) indicate the significant interconnectivity of the ions. For example, ≈30% of Cl anions interact with at least two first

Table 7. Average Percentage of Chloride Anions Forming 0–5 Hydrogen Bonds with Each Hydrogen Atom Type, Using an Angular Cutoff of 60°

	0-HB (%)	1-HB (%)	2-HB (%)	3-HB (%)	4-HB (%)	5-HB (%)
[C ₄ C ₁ im]Cl						
HCR···Cl ⁻	27.33	44.36	23.30	4.46	0.55	0.00
HW1···Cl ⁻	34.71	40.70	18.74	5.21	0.64	0.00
HW2···Cl ⁻	31.51	45.61	18.68	4.08	0.12	0.00
HMe···Cl ⁻	15.98	27.84	27.05	17.42	8.38	3.33
HC1···Cl ⁻	15.55	34.50	31.03	13.72	4.17	1.03
HC2···Cl ⁻	32.72	40.68	19.50	5.79	1.16	0.15
HCS···Cl ⁻	74.60	22.14	2.97	0.27	0.02	0.00
HCT···Cl ⁻	58.40	32.10	8.20	1.18	0.11	0.01
[C ₂ C ₁ im]Cl						
HCR···Cl ⁻	29.80	43.09	21.95	4.75	0.40	0.01
HW1···Cl ⁻	36.26	40.97	18.06	4.16	0.52	0.03
HW2···Cl ⁻	37.81	39.93	17.86	3.96	0.42	0.02
HMe···Cl ⁻	4.81	18.21	29.52	26.47	15.17	5.82
HC1···Cl ⁻	18.78	35.52	28.55	12.82	3.64	0.69
HC2···Cl ⁻	16.79	32.83	28.60	15.05	5.35	1.38

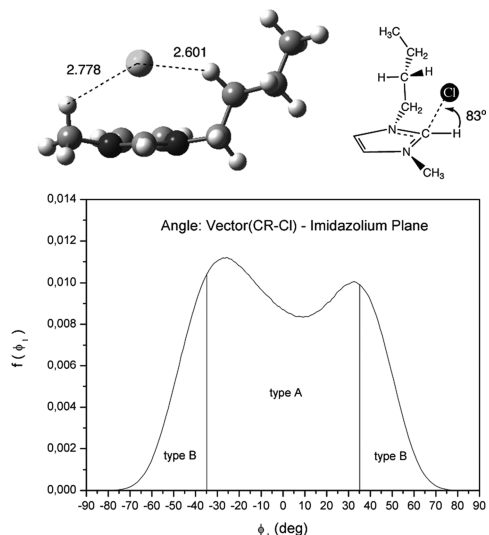


Figure 11. (a) Cl anion “top” position determined at the MP2/6-311+G(d,p) level; (b) distribution of the angles ϕ_1 , defined between the $(CR\cdots Cl^-)$ vector and the imidazolium plane for atoms within the cutoff distances $R_{H\cdots Cl}$ and $R_{C\cdots Cl}$ and within the cutoff angle of 60° for $[C_4C_1im]Cl$.

hydrogen atoms (from different cations). In addition, Cl anions on average form multiple interactions with first rather than ring hydrogen atoms; see the italic area of Table 7. In contrast, the fraction of Cl anions forming multiple H-bonds with alkyl hydrogen atoms is very small. The 0-HB(%) column indicates that on average $\approx 30\%$ of Cl anions form no H-bond with ring hydrogen atoms; this number is essentially halved in the case of the first hydrogen atoms, as only $\approx 15\%$ of Cl anions have no interaction with a methylene or methyl H-atom.

Thus, the key point originating from this analysis is that (while it is well-known that the primary hydrogen atoms are important in forming one (strong) H-bond with the Cl anions) it appears that the first and second hydrogen atoms also play a very important role in maintaining the H-bonding network. Moreover, we have been able to quantify these interactions.

F. The Cl Anion Out-of-Plane Configurations. In addition to the more directional interaction of cation hydrogen to anion, these ILs exhibit “top” and “bottom” conformers where the Cl anion sits not roughly in-plane, but above or below the imidazolium ring. Ab initio structures show a more pronounced interaction with the primary C–H bond region than the center of the ring; the Cl atom lies directly above or below the middle of the C–H bond vector, Figure 11.⁴³

To further investigate the interactions around CR (as opposed to those involving the HCR hydrogen atom), additional analysis has been carried out on structures within the H-bonding CR···Cl⁻ and HCR···Cl⁻ radial cutoffs (Table 1) and Cl⁻···C–H 60° angular cutoff. The angle ϕ formed by the intersection of the CR···Cl⁻ vector with the imidazolium plane for $[C_4C_1im]Cl$ has been computed, and the distribution of ϕ is presented in Figure 11. Interactions have been divided into type A, those that are roughly “in-plane” (ϕ in the range -35° to $+35^\circ$), and type B, those that are “out-of-plane” (ϕ exhibits higher angles). Configurations are split $\approx 67:33$ between type A (in-plane) and type B (out-of-plane). A similar analysis for the rear ring carbon atoms showed no propensity for out-of-plane conformations, indicating that the charge on the CR–H unit and perhaps the ability of the anion to sit between hydrogen atoms of the methyl and butyl chain (a configuration not possible above the rear C–H bond vectors) stabilize this conformation. The presence of the out-of-plane interactions ties in well with the higher than expected interaction of Cl anions with the HC2 of the alkyl chain.

The out-of-plane conformers could potentially be the result of an interaction with the pi cloud of the imidazolium ring. Anion–π interactions are known; they include favorable nonconvalent contacts between electron deficient (π -acidic) aromatic systems (typically fluorinated aromatic rings) and an anion. Such interactions are important in supramolecular chemistry.⁸³ In the case of the imidazolium cation, the aromatic system is π -acidic due to the positive charge; we denote this a $\pi^+\cdots Cl^-$ interaction. Anion–π interactions are known to be a balance between electrostatics (interaction of the anion with a permanent quadrupole moment) and dispersion (anion-induced polarization).⁸³ Thus, is this an interaction with the aromatic electron density of the ring (quadrupole, dispersion), or more specifically an interaction with the C–H “bond” (electrostatic)? Or is there a contribution from the first and second hydrogen atoms from the alkyl groups as indicated in Figure 11? A pure $\pi^+\cdots Cl^-$ interaction is not a H-bonding interaction; however, an interaction which involves hydrogen atoms as key components might be considered a H-bonding interaction (if of an unusual type).

Undertaking a detailed investigation is outside the scope of this paper; however, we have undertaken a limited analysis. The amount of dispersion recovered in ab initio calculations increases when employing the B3LYP, B97D, and MP2 methods. The advantage of ab initio methods is the inclusion of quadrupole and anion polarization effects. We examined the Cl anion position (above the bond vector) for each of these methods and found that it shifts increasingly toward the C atom (and the ring) as more dispersion is recovered; C–H···Cl⁻ angles are 69° , 76° , and 83° , respectively. Thus, the ab initio results determine a larger out-of-plane angle than observed in the molecular dynamics. As a further complication to interpretation, all of the ab initio optimized structures exhibited concomitant rotation of the alkyl chain torsion angle (to apparently facilitate a HC2···Cl⁻ H-bond interaction (2.600

\AA at the MP2 level)). Ab initio calculations also show that orbital delocalization does extend into this region, and NBO charges indicate that both the C and the H atom are highly positively charged.^{21,42}

The key point here is that the out-of-plane structures may not be pure anion- π interactions; there may be contributions from hydrogen atoms, via the positively charged C-H “unit” and in the potential for H-bonding interactions with the alkyl chain hydrogen atoms. The nature of this interaction is complex and would benefit from further investigation.

G. Analysis Using the New Definition. The probability density distributions for the different types of H-bond length have been calculated employing the H-bonding radial cutoffs (Table 1) and an angular cutoff of 60° , Figures 12 and 13, for $[\text{C}_4\text{C}_1\text{im}]\text{Cl}$ and $[\text{C}_2\text{C}_1\text{im}]\text{Cl}$, respectively. The distributions

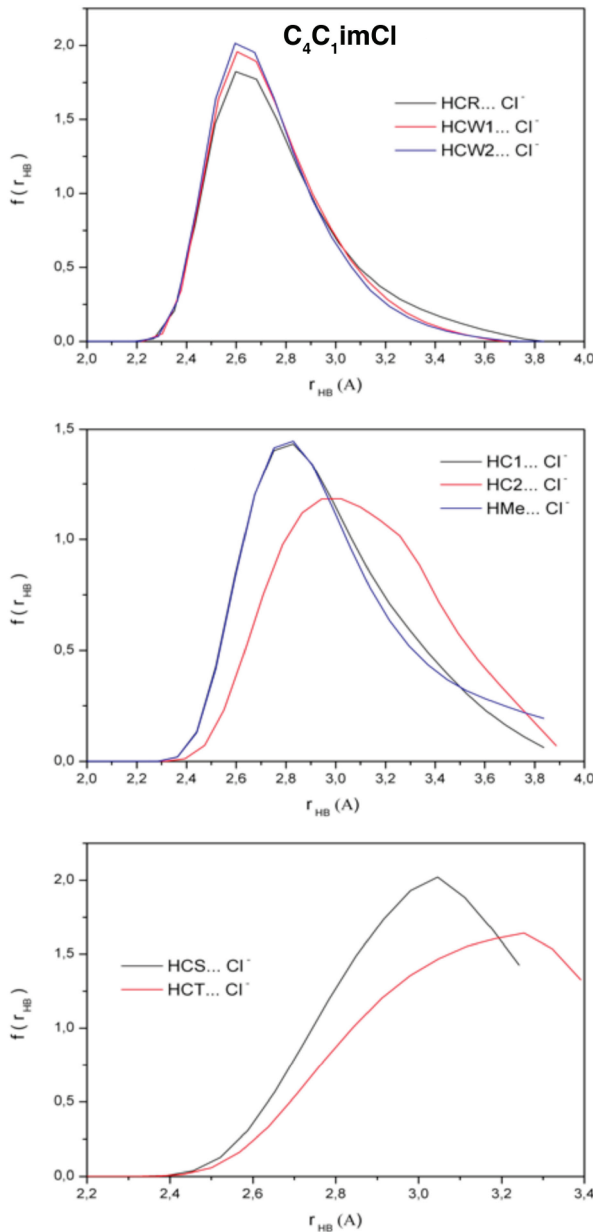


Figure 12. Distribution of hydrogen bond lengths $r(\text{H}\cdots\text{Cl}^-)$ for atoms within the cutoff distances $R_{\text{H}\cdots\text{Cl}}$ and $R_{\text{C}\cdots\text{Cl}}$ and within the cutoff angle of 60° for $[\text{C}_4\text{C}_1\text{im}]\text{Cl}$.

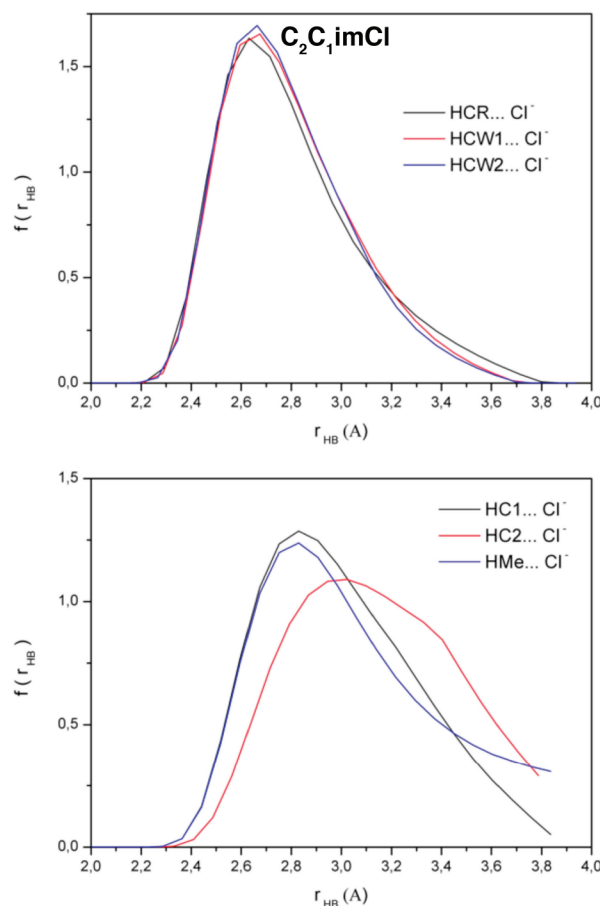


Figure 13. Distribution of hydrogen bond lengths $r(\text{H}\cdots\text{Cl}^-)$ for atoms within the cutoff distances $R_{\text{H}\cdots\text{Cl}}$ and $R_{\text{C}\cdots\text{Cl}}$ and within the cutoff angle of 60° for $[\text{C}_2\text{C}_1\text{im}]\text{Cl}$.

are sharper and the peak positions are located at smaller $\text{H}\cdots\text{Cl}^-$ distances for the primary and first compared to the alkyl hydrogen atoms. There is no substantial difference in the distributions for the primary and back ring H-bonds. Peak maxima are compared in Figure 14; as the distance from the imidazolium ring becomes larger the “most probable” H-bond length becomes longer. Ring and first H-bonds for ab initio

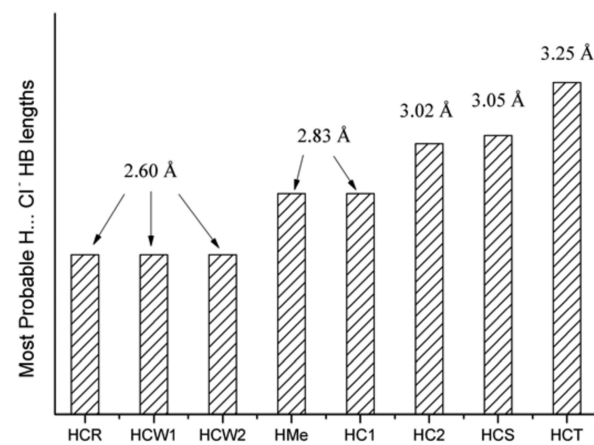


Figure 14. Graph comparing the position of the peak maxima from the hydrogen bond distance distributions, for each hydrogen atom type in $[\text{C}_4\text{C}_1\text{im}]\text{Cl}$.

isolated momomers occur at ≈ 2.00 – 2.17 and 2.35 – 2.50 , respectively,⁴³ thus, in the liquid environment there is an increase in H-bond length of roughly 0.5 Å. Thus, an analysis of H-bonding employing the new wider angle criteria reproduces the expected trends, consistent with the general understanding of these ILs. It is in analysis of the details that we have found new insight and a number of surprising results.

H. Temperature Effects on $[C_2C_1im]$. The simulations for $[C_4C_1im]Cl$ are run for a density of 1052.8 kg m⁻³ at 353.15 K close to the melting point ($T_m = 340.1$ K), while those for $[C_2C_1im]Cl$ are run for a density of 1040.0 kg m⁻³ at a higher temperature 450.0 K, well above the melting point ($T_m = 360.0$ K). Comparing results from the $[C_4C_1im]Cl$ and $[C_2C_1im]Cl$ simulations provides information on the effects of a more fluid environment (less dense, higher temperature). Aside from the expected geometric differences (ethyl to butyl chain), the results in terms of H-bonding are remarkably similar for both $[C_4C_1im]Cl$ and $[C_2C_1im]Cl$, despite the temperature being almost 100 K higher for $[C_2C_1im]Cl$.

More subtle differences can be found; for example, peak intensities for the calculated hydrogen and carbon based prdfs of $[C_2C_1im]Cl$ are lower than those for $[C_4C_1im]Cl$, indicating that at higher temperatures and lower densities these interactions become weaker. The angle distributions for $[C_2C_1im]Cl$ are slightly wider, and peaks are located at slightly larger angles; this behavior is similar to that observed for water and alcohols on heating. The average numbers of H-bonds in $[C_2C_1im]Cl$ are almost the same as in $[C_4C_1im]Cl$. Moreover, the peak positions and average H-bonding distances (Table 8) are only slightly larger than those obtained for $[C_4C_1im]Cl$.

Table 8. Mean Hydrogen Bond Length $\langle r_{HB} \rangle$ and Peak Maxima λ (Most Probable Hydrogen Bond Length) in Å for the Hydrogen Bond Distributions Evaluated When All Atoms Lie within the Cutoff Distances for $R_{H\cdots Cl^-}$ and $R_{C\cdots Cl^-}$ and Using an Angular Cutoff of 60° for $[C_4C_1im]Cl$ and $[C_2C_1im]Cl$

	$[C_4C_1im]$		$[C_2C_1im]$	
	λ (Å)	$\langle r_{HB} \rangle$ (Å)	λ (Å)	$\langle r_{HB} \rangle$ (Å)
HCR \cdots Cl $^-$	2.60	2.78	2.63	2.80
HW1 \cdots Cl $^-$	2.60	2.75	2.67	2.80
HW2 \cdots Cl $^-$	2.60	2.74	2.66	2.79
HMe \cdots Cl $^-$	2.83	2.99	2.83	3.04
HC1 \cdots Cl $^-$	2.83	2.97	2.83	3.00
HC2 \cdots Cl $^-$	3.02	3.11	3.02	3.13
HCS \cdots Cl $^-$	3.05	2.98	—	—
HCT \cdots Cl $^-$	3.25	3.08	—	—

In order to confirm this picture of temperature effects on H-bond structure, $[C_2C_1im]Cl$ was also simulated at a lower temperature, slightly above its melting point (363 K) at the corresponding experimental density.⁶⁹ The mean number of H-bonds (determined using both radial cutoffs and an angular cutoff of 60°) for the ring hydrogen atoms have been calculated and compared to the results obtained at the higher temperature. As expected, given the small differences for different ILs, the temperature effects on the H-bond structure for the same IL are not significant. A very small decrease of the average number of H-bonds has been observed on going from the lower to the higher temperature. The mean number of H-bonds per HCR atom decreases from 1.08 at 363 K to 1.03 at 450 K. In the case

of HCW1, the mean number of H-bonds decreases from 1.00 to 0.92, and for HCW1 it decreases from 1.00 to 0.90.

Therefore, it appears that the static H-bonding network has not been significantly affected by the temperature and density changes over the range investigated here. Nevertheless, transport and dynamic properties of ILs are affected by temperature changes.^{17,82} At a molecular level, properties such as viscosity and conductivity can be linked to the H-bonding interactions in ILs,^{22,35} thus linking changes in temperature with changes in H-bonding within ILs. As the static H-bonding network does not appear to be significantly effected by the temperature and density changes, it is likely that the dynamics, or breaking and reforming, of H-bonds within the liquid is important. Thus, we are now investigating the effects of temperature on the dynamic H-bonding for these ILs.

IV. CONCLUDING REMARKS

A detailed investigation of H-bonding within the framework of molecular dynamics simulations of $[C_4C_1im]Cl$ and $[C_2C_1im]Cl$ has been undertaken. In analogy to determining the criteria for H-bonding in water and alcohols, not only have distance criteria for $r(H\cdots Cl^-)$ been examined but also those for the $r(C\cdots Cl^-)$ distance and the $\phi(Cl^- \cdots C-H)$ angle have been evaluated. Employing all three criteria provide for a robust analysis. The range and type of H-bonding interactions in $[C_4C_1im]Cl$ and $[C_2C_1im]Cl$ is large, and while the first minima of the atom–atom radial distribution functions provide good distance based cutoff criteria, the situation for the angular distribution cutoff is significantly more complex. The number of H-bonds per hydrogen atom (or Cl anion) is highly angle dependent. We have found that the qualitative interpretation of H-bonding changes significantly with cutoff angle, and analyzing just one cutoff angle can give an incomplete picture of the H-bonding in these ILs. An angular cutoff of 30° may be too restrictive, as it does not include the bulk of the angle distribution for interactions that satisfy both distance criteria, and it does not reproduce the generally accepted picture of H-bonding within these ILs. We provide evidence for considering 60° as an alternative cutoff for imidazolium based ILs.

An extensive analysis of the H-bonds formed by each type of hydrogen atom (ring, first, or alkyl) has been presented. We have quantified the number of H-bonds formed by each hydrogen atom and by the Cl anion as a H-bond acceptor. This has shown that the ring hydrogen atoms typically form a single strong H-bond with a Cl anion, or in a small percentage of cases one hydrogen atom participates in two H-bonds (5–10%). The Cl anion has shown a high level of interconnectivity, forming multiple H-bonds; on average these are well distributed over all the types of hydrogen atom and even with the HC2, only the terminus of the longer alkyl group is avoided.

A key new insight obtained from our data is that the first hydrogen atoms (in the methylene and methyl groups attached directly to the nitrogen atoms) impact significantly on H-bond networking within the ionic liquid, and a larger percentage of Cl anions coordinate to multiple cations via these first hydrogen atoms. The methyl group interactions are of particular interest as they are prominent in the molecular dynamics simulation, but not in isolated ion pairs, indicating the methyl substituent hydrogen atoms offer an important secondary networking and stabilizing effect found primarily in the liquid phase. Moreover, the first and second hydrogen atoms pull Cl anions away from linear H-bonds with the primary hydrogen atoms, contributing

to the wider angle distribution. These hydrogen atoms may also contribute to stabilization of the top and bottom anion–π conformers. On average ≈70–80% of the first hydrogen atoms are involved in the formation of one or more H-bonds (Table 6), and as there are more of these (2 for the methylene group and 3 for the methyl group) contributions are large.

Finally, an increase in temperature of 100 K does not significantly affect the average number of H-bonds formed by each type of hydrogen atom; interestingly, this indicates that temperature has a larger effect on the H-bond dynamics than on the static distribution or network of H-bonds with in these ILs.

AUTHOR INFORMATION

Corresponding Author

*E-mail: i.skarmoutsos@imperial.ac.uk (I.S.), p.hunt@imperial.ac.uk (P.A.H.).

Notes

The authors declare no competing financial interest.

ACKNOWLEDGMENTS

I.S. acknowledges the postdoctoral financial support provided through an ERC Advanced Investigator Grant held by Prof. Welton and Dr. Hunt, and Professor Agílio Pádua (Université Blaise Pascal Clermont-Ferrand, France) for providing useful information about the force fields of the investigated ionic liquids. P.A.H. gratefully acknowledges The Royal Society for a University Research Fellowship.

REFERENCES

- (1) (a) Wasserscheid, P.; Wilhelm, K. *Angew. Chem.* **2000**, *112*, 3296. (b) Wasserscheid, P.; Wilhelm, K. *Angew. Chem., Int. Ed.* **2000**, *39*, 3772.
- (2) Welton, T. *Chem. Rev.* **1999**, *99*, 2071.
- (3) (a) *Ionic Liquids in Synthesis*; Welton, T., Wasserscheid, P., Eds.; Wiley-VCH: Weinheim, Germany, 2003. (b) *Ionic Liquids in Synthesis*, 2nd ed.; Welton, T., Wasserscheid, P., Eds.; Wiley-VCH: Weinheim, Germany, 2007.
- (4) *Ionic Liquids: Industrial Applications for Green Chemistry*; Rogers, R. D., Seddon, K. R., Eds.; American Chemical Society: Washington, DC, 2002; Vol. 818.
- (5) *Ionic Liquids as Green Solvents: Progress and Prospects*; Rogers, R. D., Seddon, K. R., Eds.; American Chemical Society: Washington, DC, 2003; Vol. 856.
- (6) Earle, M. J.; Mc Cormac, P. B.; Seddon, K. R. *Chem. Commun.* **1998**, *20*, 2245.
- (7) Fuller, J.; Carlin, R. T.; Osteryoung, R. A. *J. Electrochem. Soc.* **1997**, *144*, 3881.
- (8) *Electrochemical Aspects of Ionic Liquids*; Ohno, H., Ed.; Wiley-Interscience: Hoboken, NJ, 2005.
- (9) Holbrey, J. D.; Seddon, K. R. *Clean Products and Processes*; Springer: Heidelberg, Germany, 1999; Vol. 1, p 223.
- (10) Wasserscheid, P. *Nature* **2006**, *439*, 797.
- (11) (a) Lynden-Bell, R. M.; Del Popolo, M. G.; Youngs, T. G. A.; Kohanoff, J.; Hanke, C. G.; Harper, J. B.; Pinilla, C. C. *Acc. Chem. Res.* **2007**, *40*, 1138. (b) Jin, H.; O'Hare, B.; Dong, J.; Arzhantsev, S.; Baker, G. A.; Wishart, J. F.; Benesi, A. J.; Maroncelli, M. *J. Phys. Chem. B* **2008**, *112*, 81.
- (12) (a) Pârvulescu, V. I.; Hardacre, C. *Chem. Rev.* **2007**, *107*, 2615. (b) Castner, E. W., Jr.; Margulis, C. J.; Maroncelli, M.; Wishart, J. F. *Annu. Rev. Phys. Chem.* **2011**, *132*, 85.
- (13) Pádua, A. A. H.; Costa Gomes, M. F.; Canongia Lopes. *Acc. Chem. Res.* **2007**, *40*, 1087.
- (14) (a) Binnemans, K. *Chem. Rev.* **2005**, *105*, 4148. (b) Hu, Z.; Margulis, C. J. *Proc. Natl. Acad. Sci. U.S.A.* **2006**, *103*, 831.
- (15) Rogers, R. D.; Seddon, K. R. *Science* **2003**, *302*, 792.
- (16) Weingärtner, H. *Angew. Chem., Int. Ed.* **2008**, *47*, 654.
- (17) Rey-Castro, C.; Vega, L. F. *J. Phys. Chem. B* **2006**, *110*, 14426.
- (18) Jeffrey, G. A. *An Introduction to Hydrogen Bonding*; Oxford University Press: Oxford, U.K., 1997.
- (19) (a) Steiner, T. *Angew. Chem., Int. Ed.* **2002**, *41*, 48. (b) Grabowski, S. *Chem. Rev.* **2011**, *111*, 2597. (c) *Hydrogen Bonding—New Insights*; Grabowski, S., Ed.; Springer: Dordrecht, The Netherlands, 2006. (d) Arunan, E.; Desiraju, G. R.; Klein, R. A.; Sadlej, J.; Scheiner, S.; Alkorta, I.; Clary, D. C.; Crabtree, R. H.; Dannenberg, J. J.; Hobza, P.; Kjaergaard, H. G.; Legon, A. C.; Mennucci, B.; Nesbitt, D. *J. Pure Appl. Chem.* **2011**, *83* (8), 1619–1636.
- (20) Kempfer, V.; Kirchner, B. *J. Mol. Struct.* **2010**, *972*, 22.
- (21) Hunt, P. A.; Kirchner, B.; Welton, T. *Chem.—Eur. J.* **2006**, *12*, 6762.
- (22) Fumino, K.; Wulf, A.; Ludwig, R. *Angew. Chem., Int. Ed.* **2008**, *47*, 8731.
- (23) Dymek, C. J.; Grossie, D. A.; Fratini, A. V.; Adams, W. W. *J. Mol. Struct.* **1989**, *213*, 25.
- (24) Thar, J.; Brehm, M.; Seitsonen, A. P.; Kirchner, B. *J. Phys. Chem. B* **2009**, *113*, 15129.
- (25) Hitchcock, P. B.; Seddon, K. R.; Welton, T. *J. Chem. Soc., Dalton Trans.* **1993**, 2639.
- (26) Del Pópolo, M. G.; Lynden-Bell, R. M.; Kohanoff, J. *J. Phys. Chem. B* **2005**, *109*, 5895.
- (27) Lynden-Bell, R. M. *Mol. Phys.* **2003**, *101*, 2625.
- (28) Zhao, W.; Leroy, F.; Heggen, B.; Zahn, S.; Kirchner, B.; Balasubramanian, S.; Müller-Plathe, F. *J. Am. Chem. Soc.* **2009**, *131*, 15825.
- (29) (a) Qiao, B.; Krekeler, C.; Berger, R.; Delle Site, L.; Holm, C. *J. Phys. Chem. B* **2008**, *112*, 1743. (b) Spickermann, C.; Thar, J.; Lehmann, S. B. C.; Zahn, S.; Hunger, J.; Buchner, R.; Hunt, P. A.; Welton, T.; Kirchner, B. *J. Chem. Phys.* **2008**, *129*, 104505. (c) Buhl, M.; Chaumont, A.; Schurhammer, R.; Wipff, G. *J. Phys. Chem. B* **2005**, *109*, 18591. (d) Bhargava, B. L.; Balasubramanian, S. *Chem. Phys. Lett.* **2006**, *417*, 486.
- (30) Gao, Y.; Zhang, L.; Wang, Y.; Li, H. *J. Phys. Chem. B* **2010**, *114*, 2828.
- (31) Dommert, F.; Schmidt, J.; Qiao, B.; Zhao, Y.; Krekeler, C.; Delle Site, L.; Berger, R.; Holm, C. *J. Chem. Phys.* **2008**, *129*, 224501.
- (32) (a) Dong, K.; Zhang, S.; Wang, D.; Yao, X. *J. Phys. Chem. A* **2006**, *110*, 9775. (b) Turner, E. A.; Pye, C. C.; Singer, R. D. *J. Phys. Chem. A* **2003**, *107*, 2277.
- (33) Zahn, S.; Thar, J.; Kirchner, B. *J. Chem. Phys.* **2010**, *132*, 124506.
- (34) Ködderman, T.; Wertz, C.; Heintz, A.; Ludwig, R. *Chem. Phys. Chem.* **2006**, *7*, 1944.
- (35) Hunt, P. A. *J. Phys. Chem. B* **2007**, *111*, 4844.
- (36) Hunt, P. A.; Gould, I. R.; Kirchner, B. *Aust. J. Chem.* **2007**, *60*, 9.
- (37) Tsuzuki, S.; Tokuda, H.; Mikami, M. *Phys. Chem. Chem. Phys.* **2007**, *9*, 4780.
- (38) Zahn, S.; Bruns, G.; Thar, J.; Kirchner, B. *Phys. Chem. Chem. Phys.* **2008**, *10*, 6921.
- (39) Hanke, C. G.; Lynden-Bell, R. M. *J. Phys. Chem. B* **2003**, *107*, 10873.
- (40) Hanke, C. G.; Atamas, N.; Lynden-Bell, R. M. *Green Chem.* **2003**, *4*, 107.
- (41) Koßmann, S.; Thar, J.; Kirchner, B.; Hunt, P. A.; Welton, T. *J. Chem. Phys.* **2006**, *124*, 174506.
- (42) Lehmann, S. B. C.; Roatsch, M.; Schöppke, M.; Kirchner, B. *Phys. Chem. Chem. Phys.* **2010**, *12*, 7473.
- (43) Hunt, P. A.; Gould, I. R. *J. Phys. Chem. A* **2007**, *110*, 2269.
- (44) Cammarata, L.; Kazarian, S. G.; Salter, P. A.; Welton, T. *Phys. Chem. Chem. Phys.* **2001**, *23*, 5192.
- (45) Saha, H.; Hamaguchi, H.-o. *J. Phys. Chem. B* **2006**, *110*, 2777.
- (46) Danten, Y.; Cabaço, M. I.; Besnard, M. *J. Phys. Chem. A* **2009**, *113*, 2873.
- (47) Elaiwi, A.; Hitchcock, P. B.; Seddon, K. R.; Srinivasen, N.; Tan, Y.-M.; Welton, T.; Zora, J. *A. J. Chem. Soc., Dalton Trans.* **1995**, 3467.

- (48) Berg, R. W.; Deetlefs, M.; Seddon, K. R.; Shim, I.; Thomson, J. M. *J. Phys. Chem. B* **2005**, *109*, 19018.
- (49) Abdul-Sada, A. K.; Elaiwi, A. E.; Greenway, A. M.; Seddon, K. R. *Eur. Mass. Spectrom.* **1997**, *3*, 245.
- (50) Avent, A. G.; Chaloner, P. A.; Day, M. P.; Seddon, K. R.; Welton, T. *J. Chem. Soc., Dalton Trans.* **1994**, 3405.
- (51) Katsyuba, S.; Zvereva, E. E.; Vidiš, A.; Dyson, P. J. *J. Phys. Chem. B* **2007**, *111*, 352.
- (52) Aparicio, S.; Alcalde, R.; Atilhan, M. *J. Phys. Chem. B* **2010**, *114*, 5795.
- (53) Wulf, A.; Fumino, K.; Ludwig, R. *Angew. Chem., Int. Ed.* **2010**, *49*, 449.
- (54) Shukla, M.; Srivastava, N.; Saha, S. *J. Mol. Struct.* **2010**, *975*, 349.
- (55) Chang, H.-C.; Jiang, J.-C.; Tsai, W.-C.; Chen, G.-C.; Lin, S. H. *J. Phys. Chem. B* **2006**, *110*, 3302.
- (56) Hardacre, C.; Holbrey, J. D.; McMath, S. E. J.; Bowron, D. T.; Soper, A. K. *J. Chem. Phys.* **2003**, *118*, 273.
- (57) Antony, J. H.; Mertens, D.; Dölle, A.; Wasserscheid, P.; Carper, W. R. *Chem. Phys. Chem.* **2003**, *4*, 588.
- (58) Remsing, R. C.; Wildin, J. L.; Rapp, A. L.; Moyna, G. *J. Phys. Chem. B* **2007**, *111*, 11619.
- (59) Dieter, K. M.; Dymek, C. J.; Helmer, N. E.; Rovang, J. W.; Wilkes, J. S. *J. Am. Chem. Soc.* **1988**, 2722.
- (60) Luzar, A.; Chandler, D. *Nature* **1996**, *379*, 55.
- (61) (a) Haughney, M.; Ferrario, M.; Mc Donald, I. R. *Mol. Phys.* **1986**, *58*, 849. (b) Teixeira, J.; Bellissent-Funel, M.-C.; Chen, S.-H. *J. Phys.: Condens. Matter* **1990**, *2*, SA105.
- (62) Guardia, E.; Laria, D.; Martí, J. *J. Phys. Chem. B* **2006**, *110*, 6332.
- (63) (a) Martí, J. *J. Chem. Phys.* **1999**, *110*, 6876. (b) Matsumoto, M. *J. Chem. Phys.* **2007**, *126*, 054503.
- (64) Smith, W.; Forester, T. R. *J. Mol. Graph.* **1996**, *14*, 136.
- (65) Raabe, G.; Köhler, J. *J. Chem. Phys.* **2008**, *128*, 154509.
- (66) BASF BasionicsTM product booklet , 2004.
- (67) Wilkes, S. J.; Levisky, J. A.; Wilson, R. A.; Hussey, C. L. *Inorg. Chem.* **1982**, *21*, 1263.
- (68) Dong, Q.; Muzny, C. D.; Kazakov, A.; Diky, V.; Magee, J. W.; Widegren, J. A.; Chirico, R. D.; Marsh, K. N.; Frenkel, M. *J. Chem. Eng. Data* **2007**, *52*, 1151.
- (69) Fannin, A. A., Jr.; Floreani, J. D. A.; King, L. A.; Landers, J. S.; Piersma, B. J.; Stech, D. J.; Vaughn, R. L.; Wilkes, J. S.; Williams, J. L. *J. Phys. Chem.* **1984**, *88*, 2614.
- (70) (a) Urahata, S. M.; Ribeiro, M. C. C. *J. Chem. Phys.* **2004**, *120*, 1855. (b) Urahata, S. M.; Ribeiro, M. C. C. *J. Chem. Phys.* **2005**, *122*, 024511.
- (71) Allen, M. P.; Tildesley, D. J. *Computer Simulations of Liquids*; Oxford University Press, Oxford, U.K., 1987.
- (72) Hoover, W. G. *Phys. Rev.* **1985**, *A31*, 1695.
- (73) Smith, W.; Forester, T. R. *Comput. Phys. Commun.* **1994**, *79*, 63.
- (74) Ryckaert, J. P.; Ciccotti, G.; Berendsen, H. J. C. *J. Comput. Phys.* **1977**, *23*, 327.
- (75) Canongia Lopes, J. N.; Deschamps, J.; Pádua, A. A. H. *J. Phys. Chem. B* **2004**, *108*, 2038.
- (76) Canongia Lopes, J. N.; Pádua, A. A. H.; Shimizu, K. *J. Phys. Chem. B* **2008**, *112*, 5039 (il. ff, Supporting Information).
- (77) Skarmoutsos, I.; Guardia, E. *J. Chem. Phys.* **2010**, *132*, 074502.
- (78) Skarmoutsos, I.; Guardia, E. *J. Phys. Chem. B* **2009**, *113*, 8898.
- (79) Holbrey, J. D.; Reichert, W. M.; Nieuwenhyzen, M.; Johnston, S.; Seddon, K. R.; Rogers, R. D. *Chem. Commun.* **2003**, 1636.
- (80) Crowhurst, L.; Mawdsley, P. R.; Perez-Arlanidis, J. M.; Salter, P. A.; Welton, T. *Phys. Chem. Chem. Phys.* **2003**, *5*, 2790.
- (81) Saha, S.; Hayashi, S.; Kobayashi, A.; Hamaguchi, H. *Chem. Lett.* **2003**, *32*, 740.
- (82) Chen, T.; Chidambaram, M.; Liu, Z.; Smit, B.; Bell, A. T. *J. Phys. Chem. B* **2010**, *114*, 5790.
- (83) Schottel, B.; Chifotides, H.; Dunbar, K. *Chem. Soc. Rev.* **2008**, *37*, 68.